

First-principles calculations of band offsets of $\text{Al}_x\text{Ga}_{1-x}\text{P} - \text{GaP}(001)$ heterostructures

This article has been downloaded from IOPscience. Please scroll down to see the full text article.

1997 J. Phys.: Condens. Matter 9 L279

(<http://iopscience.iop.org/0953-8984/9/18/005>)

View [the table of contents for this issue](#), or go to the [journal homepage](#) for more

Download details:

IP Address: 171.66.16.207

The article was downloaded on 14/05/2010 at 08:35

Please note that [terms and conditions apply](#).

LETTER TO THE EDITOR

First-principles calculations of band offsets of $\text{Al}_x\text{Ga}_{1-x}\text{P-GaP}(001)$ heterostructuresS J Chua^{†‡}, X H Zhang[†], S J Xu[‡] and X Gu[†][†] Center for Optoelectronics, Department of Electrical Engineering, National University of Singapore, 10 Kent Ridge Crescent, Singapore 119260[‡] Institute of Materials Research and Engineering, National University of Singapore, 10 Kent Ridge Crescent, Singapore 119260

Received 3 March 1997

Abstract. A first-principles pseudopotential method combined with the virtual-crystal approximation (VCA) is used to calculate band offsets of $\text{Al}_x\text{Ga}_{1-x}\text{P-GaP}(001)$ heterostructures. It was found that both the valence and conduction band offsets vary linearly with the alloy composition. Our results are in good agreement with the experimental data.

Semiconductor superlattices and quantum wells are of considerable technological importance because of their great flexibility in tailoring electronic properties of semiconductor devices. The valence and conduction band offsets (VBOs and CBOs) are fundamental parameters which determine the physical properties of these heterostructures. Both model theories [1–5] and first-principles theories [6–13] have been developed to determine the band offset. Model theories rely on information about the bulk alone, and do not provide a complete description of the electron distribution at the interface. The only way to obtain a full picture of this effect is to perform a calculation in which the electrons are allowed to adjust to the specific environment created by the interface. This can be accomplished by performing self-consistent first-principles calculations, which will correctly describe the electrostatic potential shift that determines the band lineups. In this respect, self-consistent first-principles calculations have shown their superiority over model theories.

AlP-GaP and $\text{Al}_x\text{Ga}_{1-x}\text{P-GaP}$ superlattices have attracted a great deal of interest [14–17] because of the possibility of creating a direct band-gap material from indirect-band-gap constituents. If the indirect-band-gap to direct-band-gap transition can be realized in $\text{Al}_x\text{Ga}_{1-x}\text{P-GaP}$ superlattices, they will become the most promising materials available for optical devices in the visible region (from green to yellow). To understand the nature and the characteristics of luminescence of $\text{Al}_x\text{Ga}_{1-x}\text{P-GaP}$, a good determination of the band lineups is very important. Morii and his coworkers [18] studied the conduction band offsets of $\text{Al}_x\text{Ga}_{1-x}\text{P-GaP}(001)$ heterojunctions by means of capacitance–voltage measurements. However, to our knowledge, there are no first-principles pseudopotential calculations on this material system so far. In this work we present results of first-principles pseudopotential calculations of VBOs of $\text{Al}_x\text{Ga}_{1-x}\text{P-GaP}(001)$ heterostructures with the virtual-crystal approximation (VCA).

Wei and Zunger [19] have discussed the treatment of the disordered ternary alloy using the VCA. They believe that, for most alloy systems, the VCA tends to underestimate the optical bowing (non-linear deviations from the composition-weighted band gaps), due to

a strong ordering potential. On the other hand, Nelson *et al* [20] have shown that the first-principles virtual-crystal calculations can yield a good description of the band offsets in the GaAs–Al_xGa_{1-x}As system since the optical bowing is small. Owing to the close matching of the lattice constants of GaP and AlP, Al_xGa_{1-x}P compounds exhibit a small difference between Ga–P and Al–P bond lengths. This suggests that, at least to a first-order approximation, one can neglect lattice distortion effects in Al_xGa_{1-x}P and assume that the atomic positions of the anion and the cation sublattices remain unchanged on going from pure compound systems GaP and AlP. When cations are randomly distributed, the resulting system is the homogeneous alloy Al_xGa_{1-x}P, which can be treated within the VCA. Thus, we believe that the use of the VCA to estimate the band offsets of Al_xGa_{1-x}P–GaP heterostructures is reasonable.

We follow the theoretical framework described in detail elsewhere [8, 9]. As usual, the VBO can be divided into two parts:

$$\text{VBO} = \Delta E_V + \Delta V. \quad (1)$$

Here ΔE_V , which is referred to as the band structure term, is the difference between two bulk material band edges, when the single-particle eigenvalues are measured with respect to the average of the electrostatic potential in each bulk material. The spin–orbit effects are included in this term. This term is however characteristic of the two individual bulks, and can be evaluated from separate calculations for the two materials. The second term ΔV in (1) is the difference between the macroscopic averaged electrostatic potential on the two sides of the interface, which contains all of the interface effects.

The macroscopic average $V_{macro}(z)$ of the potential $V(x, y, z)$ throughout the heterojunction is obtained from the relations

$$V_{macro}(z) = \int_{-d/4}^{+d/4} dz' \bar{V}(z + z') \quad (2)$$

$$\bar{V}(z) = \frac{1}{A} \int_A dx dy V(x, y, z) \quad (3)$$

where d is the lattice constant and $\bar{V}(z)$ is a planar-averaged potential, i.e., the full potential $V(x, y, z)$ averaged over a two-dimensional unit cell A in a plane parallel to the interface. Far from the interface, this planar-averaged potential $\bar{V}(z)$ is periodic over a distance $d/2$. This is a relation of the fact that the charge density far from the interface is identical to that of the bulk material, and therefore the potential in this region must be identical to the potential of the bulk material to within a constant. The macroscopic-averaged potential as defined in (2) is thus a constant far from the interface, and the difference in the constant values on either side of the interface is simply ΔV .

The calculations are performed within the framework of density functional theory (DFT) [21, 22] with the local density approximation (LDA), applied in the momentum space formalism [23], using non-local norm-conserving pseudopotentials [24], and a plane-wave basis set. For the exchange–correlation potential we use the Ceperley–Alder [25] form of the LDA as parametrized by Perdew and Zunger [26]. The Brillouin zone (BZ) integrations are performed by sampling on a regular Monkhorst–Pack (MP) mesh [27] in reciprocal space, which is equivalent to using Chadi–Cohen special points [28].

The bulk band structure calculations were performed using the zinc-blende unit cell. The Brillouin zone integrations were performed by sampling on a regular (444) MP mesh in reciprocal space, which is equivalent to using ten special points. The wavefunctions were expanded in a plane wave basis set including all plane waves up to 16 Ryd in kinetic energy. For the potential lineup term, the calculations were performed based on

$(\text{Al}_x\text{Ga}_{1-x}\text{P})_3(\text{GaP})_3(001)$ superlattice geometry where all the atoms occupy the sites of a perfect tetragonal lattice whose lattice constant $d = 5.456 \text{ \AA}$ is the average of the experimental lattice constants of AlP and GaP. The basis set consists of plane waves with a kinetic energy cutoff of 9.0 Ryd and the (444) MP cubic mesh appropriately folded for this geometry (equivalent to using eight special points) is used to perform k -space integrations. To check that the two interfaces in our supercell are sufficiently far apart to be decoupled, the macroscopic averaged charge density $n_{macro}(z)$ and the macroscopic averaged potential $V_{macro}(z)$ for the $(\text{AlP})_3(\text{GaP})_3(001)$ superlattice are plotted in figure 1. The flatness of $n_{macro}(z)$ and $V_{macro}(z)$ far from the interfaces indicates our supercell is long enough to recover the bulk features midway between the two interfaces. Similar results hold for other alloy compositions. We have also performed convergence tests with different MP meshes and kinetic energy cutoff values and estimate our relative numerical accuracy to be approximately 0.03 eV.

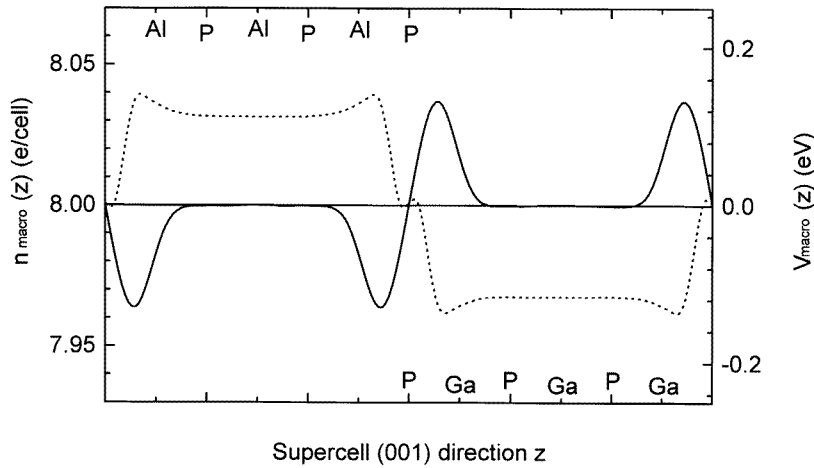


Figure 1. The macroscopic averaged charge density (solid line) and macroscopic averaged electrostatic potential (dotted line) of the $(\text{AlP})_3(\text{GaP})_3(001)$ supercell plotted in the direction normal to the interface.

Combining the band structure term and potential lineup term, the VBO can be obtained. However, the determination of the CBOs is not straightforward, since the band gaps are underestimated within the LDA. Thus the following equation [29] was used to describe the indirect band gaps of $\text{Al}_x\text{Ga}_{1-x}\text{P}$:

$$E_{g, ind} = 2.28 + 0.16x. \quad (4)$$

Combining with the relationship $\Delta E_g = \text{VBO} + \text{CBO}$, the CBOs can be determined. The calculated VBOs and derived CBOs with various Al compositions are plotted in figure 2 and summarized in table 1. For the whole composition range, $\text{Al}_x\text{Ga}_{1-x}\text{P}$ -GaP heterostructures have type II alignments with the band edge of GaP lying higher than that of $\text{Al}_x\text{Ga}_{1-x}\text{P}$. It is noted that both VBOs and CBOs increase linearly with increasing Al composition x .

For the AlP-GaP(001) heterojunction, the calculated VBO is 0.42 eV. Using experimental band gap energies of 2.45 and 2.27 eV for AlP and GaP, respectively, we obtain a CBO of 0.24 eV, which is in very good agreement with the CBO = 0.23 eV, experimentally obtained by Morii and his coworkers [18].

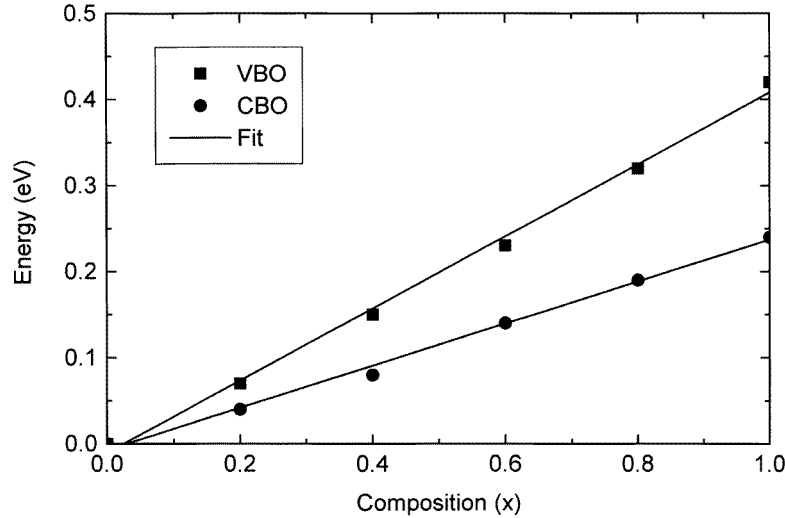


Figure 2. The valence and conduction band offsets of $\text{Al}_x\text{Ga}_{1-x}\text{P-GaP}(001)$ heterostructures with various Al compositions. The linear fitted lines are also plotted.

Table 1. Calculated valence and conduction band offsets (VBOs and CBOs) including the spin-orbit interaction.

Structure	VBO (eV)	CBO (eV)
$\text{Al}_{0.2}\text{Ga}_{0.8}\text{P-GaP}$	0.07	0.04
$\text{Al}_{0.4}\text{Ga}_{0.6}\text{P-GaP}$	0.15	0.08
$\text{Al}_{0.6}\text{Ga}_{0.4}\text{P-GaP}$	0.23	0.14
$\text{Al}_{0.8}\text{Ga}_{0.2}\text{P-GaP}$	0.32	0.19
AlP-GaP	0.42	0.24 (0.23) ^a

^a Experimental value [18].

In conclusion, we have shown by means of self-consistent first-principles virtual-crystal calculations that both the valence and conduction band offsets depend linearly on the alloy composition in $\text{Al}_x\text{Ga}_{1-x}\text{P-GaP}(001)$ heterostructures. This confirms, *a posteriori*, that the first-principles pseudopotential method combined with the VCA can yield a good description of band offsets for this system.

We would like to acknowledge the Computer Center and the National Supercomputing Research Center, National University of Singapore (NUS), for the use of supercomputers. X H Zhang also acknowledges NUS for providing a research studentship.

References

- [1] Harrison W A 1977 *J. Vac. Sci. Technol.* **14** 1016
- [2] Tersoff J 1984 *Phys. Rev. Lett.* **52** 465
- [3] Tersoff J 1984 *Phys. Rev. B* **30** 4874
- [4] Cardona M and Kleinman L 1987 *Phys. Rev. B* **35** 6182
- [5] Van de Walle C G 1989 *Phys. Rev. B* **39** 1871
- [6] Van de Walle C G and Martin R M 1985 *J. Vac. Sci. Technol. B* **3** 1256
Van de Walle C G and Martin R M 1986 *J. Vac. Sci. Technol. B* **4** 1055

- Van de Walle C G and Martin R M 1986 *Phys. Rev. B* **34** 5621
Van de Walle C G and Martin R M 1987 *Phys. Rev. B* **35** 8154
- [7] Bylander D M and Kleinman L 1987 *Phys. Rev. Lett.* **59** 2091
Bylander D M and Kleinman L 1987 *Phys. Rev. B* **36** 3229
- [8] Baldereschi A, Baroni S and Resta R 1988 *Phys. Rev. Lett.* **61** 734
- [9] Baroni S, Resta R, Baldereschi A and Peressi M 1989 *Spectroscopy of Semiconductor Microstructures (NATO Advanced Study Institute, Series B: Physics 106)* ed G Fasol, A Fasolino and P Lugli (New York: Plenum) pp 251, 271
- [10] Resta R, Colombo L and Baroni S 1990 *Phys. Rev. B* **41** 12358
Resta R, Colombo L and Baroni S 1991 *Phys. Rev. B* **43** 14273
- [11] Colombo L, Resta R and Baroni S 1991 *Phys. Rev. B* **44** 5572
- [12] Qteish A and Needs R J 1990 *Phys. Rev. B* **42** 3044
Qteish A and Needs R J 1991 *Phys. Rev. B* **43** 4229
- [13] Tit N, Peressi M and Baroni S 1993 *Phys. Rev. B* **48** 17607
- [14] Park C H and Chang K J 1993 *Phys. Rev. B* **47** 12709
- [15] Asami K, Asahi H, Watanabe T, Enokida M and Gonda S 1993 *Appl. Phys. Lett.* **62** 81
- [16] Issiki F, Fukatsu S and Shiraki Y 1995 *Appl. Phys. Lett.* **67** 1048
- [17] Suto K, Agachi S, Yoneyama T and Nishizawa J 1996 *J. Cryst. Growth* **160** 13
- [18] Morii A, Okagawa H, Hara K, Yoshino J and Kukimoto H 1992 *Japan. J. Appl. Phys.* **31** L1661
- [19] Wei S H and Zunger A 1989 *Phys. Rev. B* **39** 3279
- [20] Nelson J S, Wright A F and Fong C Y 1991 *Phys. Rev. B* **43** 4908
- [21] Hohenberg P and Kohn W 1964 *Phys. Rev.* **136** B864
- [22] Kohn W and Sham L J 1965 *Phys. Rev.* **140** A1133
- [23] Ihm J, Zunger A and Cohen M L 1979 *J. Phys. C.: Solid State Phys.* **12** 4409
- [24] Hamann D R, Schlüter M and Chiang C 1979 *Phys. Rev. Lett.* **43** 1494
- [25] Ceperley D M and Alder B J 1980 *Phys. Rev. Lett.* **45** 566
- [26] Perdew J and Zunger A 1981 *Phys. Rev. B* **23** 5048
- [27] Monkhorst H J and Pack J D 1976 *Phys. Rev. B* **13** 5188
- [28] Chadi D J and Cohen M L 1973 *Phys. Rev. B* **8** 5747
- [29] *Landolt-Börnstein New Series* 1987 vol 22a, ed O Madelung (Berlin: Springer)